Cementoblast Delivery for Periodontal Tissue Engineering

Ming Zhao,* Qiming Jin,* Janice E. Berry,* Francisco H. Nociti Jr.,† William V. Giannobile,* and Martha J. Somerman‡

Background: Predictable periodontal regeneration following periodontal disease is a major goal of therapy. The objective of this proof of concept investigation was to evaluate the ability of cementoblasts and dental follicle cells to promote periodontal regeneration in a rodent periodontal fenestration model.

Methods: The buccal aspect of the distal root of the first mandibular molar was denuded of its periodontal ligament (PDL), cementum, and superficial dentin through a bony window created bilaterally in 12 athymic rats. Treated defects were divided into three groups: 1) carrier alone (PLGA polymer sponges), 2) carrier + follicle cells, and 3) carrier + cementoblasts. Cultured murine primary follicle cells and immortalized cementoblasts were delivered to the defects via biodegradable PLGA polymer sponges, and mandibulae were retrieved 3 weeks and 6 weeks post-surgery for histological evaluation. *In situ* hybridization, for gene expression of bone sialoprotein (BSP) and osteocalcin (OCN), and histomorphometric analysis were further done on 3-week specimens.

Results: Three weeks after surgery, histology of defects treated with carrier alone indicated PLGA particles, fibrous tissue, and newly formed bone scattered within the defect area. Defects treated with carrier + follicle cells had a similar appearance, but with less formation of bone. In contrast, in defects treated with carrier + cementoblasts, mineralized tissues were noted at the healing site with extension toward the root surface, PDL region, and laterally beyond the buccal plate envelope of bone. No PDL-bone fibrous attachment was observed in any of the groups at this point. *In situ* hybridization showed that the mineralized tissue formed by cementoblasts gave strong signals for both BSP and OCN genes, confirming its nature as cementum or bone. The changes noted at 3 weeks were also observed at 6 weeks. Cementoblast-treated and carrier alone-treated defects exhibited complete bone bridging and PDL formation, whereas follicle cell-treated defects showed minimal evidence of osteogenesis. No new cementum was formed along the root surface in the above two groups. Cementoblast-treated defects were filled with trabeculated mineralized tissue similar to, but more mature, than that seen at 3 weeks. Furthermore, the PDL region was maintained with well-organized collagen fibers connecting the adjacent bone to a thin layer of cementum-like tissue observed on the root surface. Neoplastic changes were observed at the superficial portions of the implants in two of the 6-week cementoblast-treated specimens, possibly due in part to the SV40-transformed nature of the implanted cell line.

Conclusions: This pilot study demonstrates that cementoblasts have a marked ability to induce mineralization in periodontal wounds when delivered via polymer sponges, while implanted dental follicle cells seem to inhibit periodontal healing. These results confirm the selective behaviors of different cell types in vivo and support the role of cementoblasts as a tool to better understand periodontal regeneration and cementogenesis. *J Periodontol 2004;75:154-161.*

KEY WORDS

Animal studies; biomimetics; cementoblasts; cementogenesis; dental follicle/anatomy and histology; periodontal regeneration; wound healing.

* Center for Craniofacial Regeneration and Department of Periodontics/Prevention/Geriatrics, University of Michigan School of Dentistry, Ann Arbor, MI.
† Department of Prosthodontics and Periodontics, Division of Periodontics, School of Dentistry at Piracicaba, UNICAMP, Piracicaba, São Paulo, Brazil; previously, Department of Periodontics, School of Dentistry, University of Washington, Seattle, WA and Center for Craniofacial Regeneration and Department of Periodontics/Prevention/Geriatrics, University of Michigan.
‡ Currently, Department of Periodontics, School of Dentistry, University of Washington; previously, Center for Craniofacial Regeneration and Department of Periodontics/Prevention/Geriatrics, University of Michigan.

Periodontal diseases are marked by destruction of periodontal support, i.e., periodontal ligament (PDL), cementum, and bone, with subsequent tooth loss if left untreated. In pursuit of treatments that can reverse this destruction, including regeneration of new bone, new cementum, and supportive PDL, increased attempts have been made to understand cellular and molecular mechanisms and factors regulating formation of these tissues during development and regeneration.[1-7]

Predictable regeneration of periodontal structures following periodontal disease is a major goal of periodontal therapy. Our group has focused on defining the cells regulating periodontal tissues during development, regeneration, and repair, i.e., cementoblasts, PDL, and dental follicle cells. In vitro, immortalized murine cementoblasts exhibited a strong ability to induce mineralization,[8,9] while immortalized murine dental follicle cells and PDL fibroblasts had minimal ability to induce mineralization.[10] When delivered subcutaneously to a severely compromised immunodeficient (SCID) mouse model via type I collagen/calcium phosphate sponges or poly (DL-lactic-co-glycolic acid) (PLGA) polymer sponges, cementoblastic cells were able to induce mineralized tissue formation at both 3 and 6 weeks, but dental follicle cells and PDL cells induced no mineral formation.[11-13] In ex vivo experiments, primary murine follicle cells and human gingival fibroblasts transduced with bone morphogenetic protein (BMP)-7 adenovirus were seeded onto PLGA or gelatin sponges and implanted into the subcutaneous pouches of SCID mice. Cells transduced with BMP-7 adenovirus formed marrow-containing ossicles, while control cells did not[14] (and unpublished data). Results from these studies suggest the need for appropriate periodontal cells and factors to induce mineral formation. These findings, coupled with new technologies to deliver cells and factors to wound sites and to monitor the healing process, led us to explore the feasibility of delivering periodontal cells to osseous defects via biodegradable polymers, and to compare the abilities of different cell types to promote regeneration of periodontal structures including bone, cementum, and a functional PDL. In the present study, we delivered murine cementoblasts and primary dental follicle cells via PLGA polymer sponges to periodontal defects prepared in immunodeficient rats and examined the ability of these cells to contribute to periodontal wound repair.

MATERIALS AND METHODS

Cell Isolation and Culture

Follicle cells. Primary follicle cells were isolated from the first molars of CD-1 mice at days 3 to 5 of postnatal development as described previously.[10,15] Briefly, using a dissecting microscope, the thin layers of dental follicle around the tooth germs of first mandibular molars were removed and subjected to enzymatic digestion (collagenase type VII 0.6 mg/ml + trypsin 0.25%)[§] for 1 hour. The cells were maintained in Dulbecco's modified Eagle's medium (DMEM)[‖] containing 10% fetal bovine serum (FBS), 100 U/ml of penicillin, and 100 µg/ml streptomycin[‖] in a humidified atmosphere of 5% CO_2 at 37°C. Under these culture conditions, epithelial cells did not survive, as confirmed by lack of expression for keratins for all cells within the culture antibody to keratin[¶] (data not shown). Cells of passage 2 were used in this study.

Cementoblasts. An immortalized murine cementoblast cell line, OC-CM, was established in our laboratory, by isolating tooth root surface cells from mice containing a transgene composed of SV40 large T-antigen (TAg) under control of the osteocalcin (OCN) promoter.[16,17] Under these conditions, only cells expressing OCN, i.e., cementoblasts and not PDL cells, survive. OC-CM 30, a subclone of the immortalized OC-CM cell population, was used for this study. Cells were maintained in DMEM plus 10% FBS and antibiotics.

Scaffold Polymer Preparation and Cell Seeding

PLGA was processed into porous foams by an established solvent-casting, particulate-leaching technique using NaCl as the pyrogen, as described previously.[18] PLGA sponges were cut into $3 \times 2 \times 1$ mm blocks, sterilized with ultraviolet light, and stored at room temperature until use. The PLGA scaffolds contain 95% porosity and pore sizes ranging from 250 to 425 µm.

Prior to transplantation in vivo, the PLGA blocks were immersed in 70% ethanol for 10 minutes, rinsed with PBS three times, and incubated in DMEM with 10% FBS at 37°C overnight. On the following day, media were removed with sterilized filter paper. One million cells were suspended in 15 µl DMEM, seeded onto each polymer block, and cultured in DMEM with 10% FBS for 24 hours in culture dishes at 37°C. Five sponges were prepared for each cell group, with carrier alone as a control. The scaffolds with or without cells were implanted into the periodontal defects of nude rats as described below.

Rat Molar Fenestration Model and Sample Randomization

This study was performed under protocols approved by the University Committee on Use and Care of Animals of the University of Michigan and was in compliance with state and federal laws.

A periodontal fenestration defect model of rodents was utilized, which was modified from the method described by King et al.[19,20] (Fig. 1A). Twelve 250 to 300 g athymic rats (Hsd:RH-rnu/rnu[#]) were used, with

§ Sigma Chemical Company, St. Louis, MO.
‖ GIBCO BRL, Gaithersburg, MD.
¶ Dako Corporation, Carpinteria, CA.
# Harlan, Indianapolis, IN.

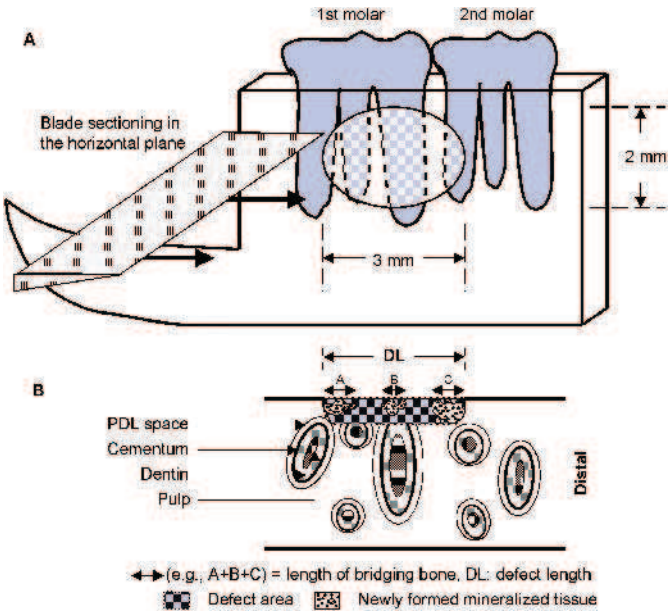

Figure 1.
Diagrams showing surgical creation of the periodontal defect ***(A)*** *and the parameters used in histomorphometric analysis* ***(B)****, modified from King et al.*[19,20]

surgical operations performed bilaterally on the mandibulae. The surgical defects were randomly assigned to one of three different therapies: 1) carrier alone, 2) carrier + follicle cells, or 3) carrier + cementoblasts and designed so that in each rat, the same treatment was not performed on both sides. Two time points, 3 and 6 weeks post-surgery, were selected for harvesting samples. Eight animals (n = 5 sites/group in an alternating split-mouth design) were analyzed at 3 weeks. An additional four animals were followed for 6 weeks to confirm stability of the findings noted at 3 weeks (two sites treated by carrier alone, two by carrier + follicle cells, and four by carrier + cementoblasts). Surgical defects were created by preparing a 2 cm superficial skin incision at the lower border of the mandible bilaterally. The superficial fascia was separated, exposing the underlying masseter muscle. The ligamentary attachment of the masseter muscle to bone was severed at its inferior base, and both the masseter and periosteum were separated from bone to expose the mandible. The oral mucosa on the superior wall of the surgically created access chamber was identified, and its attachment to the intraoral keratinized gingival margin was ensured while the tissues were retracted by periosteal elevators. The bone overlying the mandibular first molar was removed at high speed under saline irrigation. The procedure was performed under a laminar flow hood using an operating microscope at 10× magnification, taking care not to perforate the oral cavity by damaging the intraoral mucosa. The distal root of the first molar was carefully denuded of its PDL, overlying cementum, and superficial dentin. The defects measured approximately 3×2 mm. PLGA polymers measuring approximately $3 \times 2 \times 1$ mm were seated onto the defects, using gentle pressure to position the implants in close approximation with the surface of the defects. The tissues were positioned with resorbable 5-0 chromic gut sutures, and the external skin incision closed with surgical staples. The animals were given 10% dextrose solution supplemented with ampicillin (268 µg/ml) daily for 7 days. The rats were sacrificed 3 weeks and 6 weeks after surgery, and block biopsies placed into Bouin's fixative** for 24 hours. The specimens were then decalcified in AFS solution (10% glacial acetic acid/1.5% formaldehyde in normal saline solution) at 4°C for 3 to 4 weeks, followed by embedding in paraffin. Ten levels of 5 µm coronal sections were prepared along the full length of the defect, with a 200 µm interval between each section. Sections were stained with hematoxylin and eosin for histological observation by light or polarized light microscopy. Sections from the mid-portion of the defects were selected for histomorphometric analysis.

In Situ *Hybridization*

In situ hybridization was done using cDNA probes for bone sialoprotein (BSP) and OCN, two established markers for mineralized tissue, to confirm newly formed mineralized tissue in the healing area. Expression of these two genes is also seen in cementoblasts in culture. Three-week tissue sections were analyzed using procedures outlined previously.[21] Both antisense and sense (control) probes (mouse BSP cDNA from Dr. M. Young, National Institutes of Health, Bethesda, MD;[22] OCN cDNA from Dr. J. Wozney, Wyeth Research, Cambridge, MA[23]) were labeled from linearized plasmids with ^{35}S-UTP using a maxiscript kit.†† After hybridization, slides were exposed to x-ray film overnight to visualize overall hybridization patterns, and then coated with a 1:1 dilution of NTB-2 emulsion‡‡ and 6M ammonium acetate, air dried and exposed at 4°C for 30 days in the presence of desiccant. Exposed slides were developed in a developer‡‡ for 4 minutes at 15°C, stopped in water, fixed,‡‡ and washed in running water. Sections were counterstained with Gill's hematoxylin and eosin, dehydrated in ethanol, cleared in xylene, and mounted with a mounting medium. Hybridization signals were visualized under dark- and light-field microscopy using a microscope.

Histomorphometric Analysis

Computer-assisted image analysis was utilized to determine the ability of cell implantation to affect periodontal tissue repair. Three-week specimens were captured using

** Polysciences, Inc., Warrington, PA.
†† Ambion, Inc., Austin, TX.
‡‡ D-19, Eastman-Kodak, Rochester, NY.

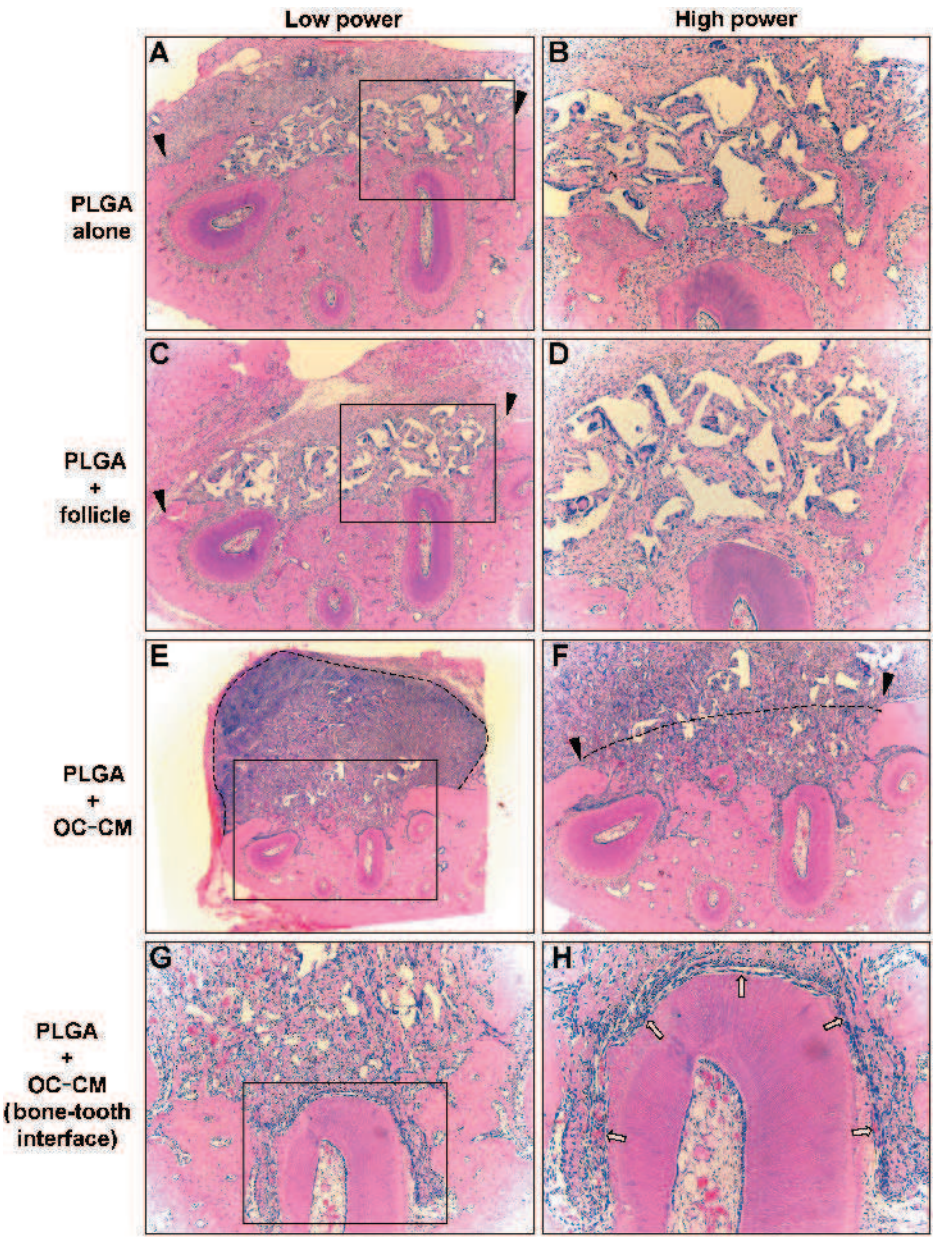

Figure 2.
Histology of periodontal healing areas 3 weeks after transplantation of PLGA sponges with or without cells (H & E staining). Arrowheads indicate the surgical margins of the defects. ***A, B)*** *PLGA carrier alone. The defect is filled with fibrous tissue and polymer particles, with newly formed bone tissue scattered within the defect (original magnification A: ×4, B: ×10).* ***C, D)*** *PLGA carrier + follicle cells. The defect contains polymer particles and fibrous tissue interspersed with numerous spindle-shaped and multinucleated cells. There is minimal evidence of new bone formation, except at the surgical margin (original magnification C: ×4, D: ×10).* ***E-H)*** *PLGA carrier + cementoblasts. Newly formed mineralized tissue with numerous blood vessels is observed filling the defect area. This tissue extends towards the PDL region and laterally beyond the envelope of the buccal plate of bone (dotted line in F). The newly formed mineralized tissue merges with surrounding bone in some areas, but is separated from the root surface by a layer of connective tissue (white arrows in H) containing spindle-shaped cells and small blood vessels (original magnification E: ×2, F: ×4, G: ×10, H: ×20).*

a light/epifluorescent microscope[§§] fitted with a camera[‖‖] and analytic software.[¶¶] A single masked, calibrated examiner (QJ) examined all of the slides and demonstrated a pre- and post-study calibration inter- and intraexaminer error of <5% compared to a standard examiner (MZ). Parameters of periodontal regeneration measured included: 1) length of defect (mm) and area of defect (mm^2); 2) length of new bridging bone measured from the border of the original osseous defect (mesially-distally) (mm); 3) total area of newly formed mineralized tissue (NM) (mm^2); 4) area of supporting NM (NM within bony envelope) (mm^2); and 5) defect fill (supporting NM area/total defect area %), as depicted in Figure 1B. Statistical analysis was performed using an analysis of variance and a Fisher's PSLD (protected least significant difference) multiple comparison procedure to measure statistical differences among groups.

RESULTS

Histology

Three-week specimens (Fig. 2). At this time point, the defects treated with carrier alone were mainly filled with fibrous tissue containing PLGA particles, with newly formed bone tissue scattered within the defects (Figs. 2A and 2B). Specimens implanted with carrier + follicle cells demonstrated similar histological features, but with less evidence of osteogenesis in the defect area (Figs. 2C and 2D). Newly formed bone tissue was

§§ Eclipse E800, Nikon, Inc., Melville, NY.
‖‖ SPOT-2, Diagnostic Instruments, Inc., Sterling Heights, MI.
¶¶ Image-Pro Plus 4.1, Media Cybernetics Inc., Silver Spring, MD.

observed mainly at the surgical margins of the lesions. PLGA scaffold residue was seen over the exposed roots in these specimens, with spindle-shaped and multinucleated cells within the fibrous tissue and at the polymer-tissue interface (Fig. 2D). In contrast, in specimens treated with carrier + cementoblasts, the defects were filled with newly formed mineralized tissue, which extended lateral to the original buccal plate and approached the PDL region (Figs. 2E and 2F). Such mineralized tissues were mainly trabeculated woven bone devoid of marrow spaces, containing numerous small blood vessels and hyperchromatic cementoblasts, similar to the mineralized tissues formed by cementoblasts implanted subcutaneously into SCID mice.[11-13] The cementoblast-formed mineralized tissue coalesced with surrounding alveolar bone in some areas, but was separated from the root surface by a layer of connective tissue containing spindle-shaped cells and small blood vessels (Figs. 2G and 2H). No formation of new cementum or a well-organized PDL was observed in specimens examined from any of the groups at this time point.

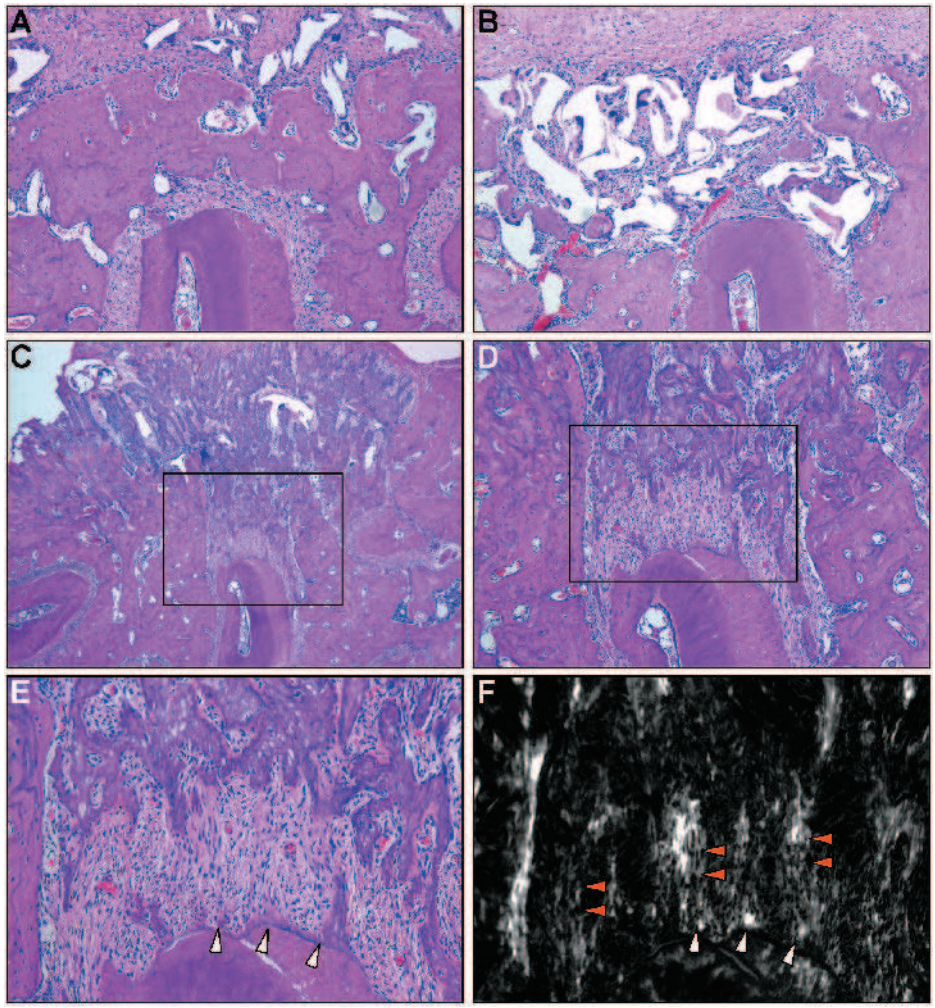

Figure 3.
Histology of periodontal healing areas 6 weeks after transplantation of PLGA sponges with or without cells (H & E staining). ***A)*** *PLGA carrier alone. Newly formed complete bone bridge is observed over the defect, with organized PDL region (original magnification ×10).* ***B)*** *PLGA carrier + follicle cells. Polymer particles are seen throughout the defect, with sparse newly formed bone fragments (original magnification ×10). No cementum formation is seen in either of the above groups.* ***C-F)*** *PLGA carrier + cementoblasts. Newly formed mineralized tissues fill the defect in a similar way to the 3-week specimens (Figs. 2E-2H). A well-organized PDL region is now seen, with organized fibers connecting the root surface and mineralized tissue. A thin layer of cementum-like tissue on the root surface is also seen (arrowheads in E). Polarized light microscopy reveals the presence of fibers consistent with nascent Sharpey's fibers emanating from the immature cemental surface (white arrow heads in F), and PDL fiber bundles (red arrow heads in F) arranged in an orientation perpendicular to cementum and alveolar bone (original magnification C: ×4, D: ×10, E and F: ×20).*

Six-week specimens (Fig. 3). At this time point, complete bone bridging was seen in the defects treated with carrier alone (n = 2) (Fig. 3A), whereas defects treated with carrier + follicle cells (n = 2) contained PLGA particles, with little newly formed bone tissue (Fig. 3B). No cementum formation was seen on the root surface in these two groups. In all specimens treated with carrier + cementoblasts (n = 4), mineralized tissues were seen filling the defects similarly to the 3-week specimens (Figs. 3C-3E). However, although limited in number, the mineralized tissues from 6-week specimens were more mature and less vascularized. Also, a well-organized PDL region was regained, showing fibers connecting the mineralized tissue and a thin layer of cementum-like tissue forming on the tooth surface (Figs. 3D and 3F). In two specimens treated with carrier + cementoblasts, neoplastic changes were noted at the superficial portion of the transplants. Histologic examination revealed increased cell density, hyperchromatism, numerous atypical mitosis, and a large number of multinucleated cells, suggesting neoplastic alteration (data not shown).

In Situ *Hybridization of BSP and OCN*

Given that the cementoblasts used here demonstrated high level expression of BSP and OCN genes prior to implantation, we sought to evaluate the expression level of these genes in the zone of the implanted cells within periodontal defects, in order to confirm the

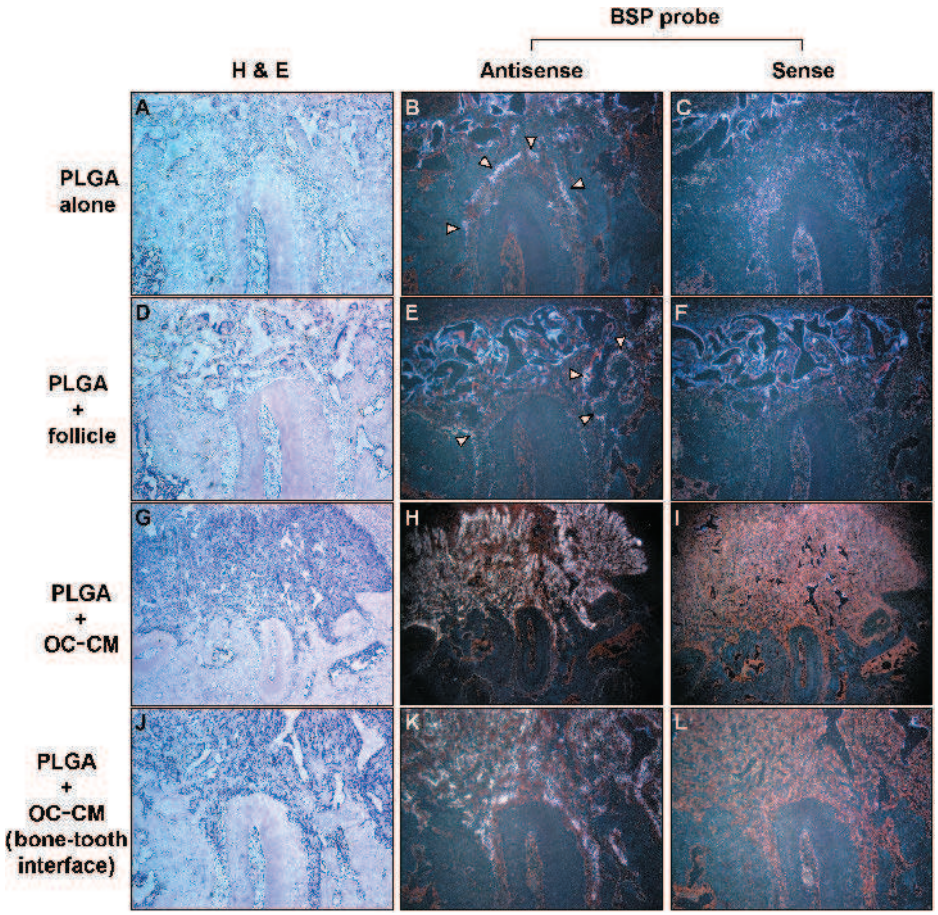

Figure 4.
In situ *hybridization with BSP probe. Left panel: H & E staining; middle panel: antisense probe; right panel: sense probe.* ***A-C)*** *PLGA alone. Strong signal is seen along the borders of newly formed bone bridge covering the defect (arrowheads) (original magnification ×10).* ***D-F)*** *PLGA + follicle cells. Limited formation of new bone is seen at the surgical margins, where positive signal is noticed (original magnification ×10).* ***G-L)*** *PLGA + cementoblasts. Strong signal is seen throughout the newly formed mineralized tissue within and outside the defect limit (original magnification G-I: × 4; J-L: ×10). No specific signal is seen in specimens exposed to sense probe. The autofluorescence seen in polymer area (A, B) is an artifact.*

bone/cementum nature of the newly formed mineralized tissue. Results of *in situ* hybridization with BSP probe (antisense and sense) on 3-week specimens are shown in Figure 4. In sections treated with carrier alone (Figs. 4A-4C), a positive signal was seen only along the borders of newly formed bone bridge over the defects. In sections treated with carrier + follicle cells (Figs. 4D-4F), a positive signal was observed only at the edge of the defects, where limited formation of new bone occurred. Autofluoresence seen in the polymer area is an artifact, which is also evident in control sections hybridized with the sense probe. In contrast, strong signals were seen in all areas of the mineralized tissues formed by implanted cementoblasts, including those encroaching into the PDL regions (Figs. 4G-4L). Hybridization with OCN probe identified a similar distribution of positive signals (not shown).

Histomorphometric Analysis

Histomorphometric analysis was done on 3-week specimens. One specimen from the carrier alone group was excluded from analysis because the polymer was found to be displaced from the defect upon histological examination. No significant differences were observed among the groups in terms of initial defect sizes and defect areas (mean range ± SD of groups): 3.12 ± 0.26 to 3.49 ± 0.21 mm and 0.97 ± 0.28 to 1.23 ± 0.28 mm^2, respectively, $P > 0.05$). Results from measuring and comparing other parameters are summarized in Figure 5. Defects treated with carrier alone and carrier + cementoblasts showed significantly greater length of bone bridging than those treated with carrier + follicle cells ($P < 0.01$). In addition, in comparison to defects treated with carrier alone and carrier + follicle cells, parameters including area of supporting NM, area of total NM, and defect fill were significantly higher in the carrier + cementoblasts group ($P < 0.01$). Carrier + follicle cells exhibited less formation of NM than the carrier-alone group in terms of defect fill ($P < 0.05$).

DISCUSSION

This "proof of concept" investigation of a limited sample set supports the notion that cementoblasts have the ability to induce mineralization in vivo in a periodontal defect and to contribute to the regenerative process. At 3 weeks post-surgery, the cementoblast-formed mineral was separated from the root surface by a layer of cell-rich connective tissue of unknown origin, and no evidence of formation of a PDL region or new cementum was observed. However, after 6 weeks, a well-organized PDL plus a layer of cementum-like tissue covering the root surface was present in the cementoblast-treated defects. The mineralized tissues formed are bone/cementum-like in that they express BSP and OCN mRNA (Figs. 4H and 4K), but the exact nature of these mineralized tissues remains to be defined. Formation of new cementum has been demonstrated previously in animal models where specific factors such as BMPs and platelet-derived growth factors were delivered to

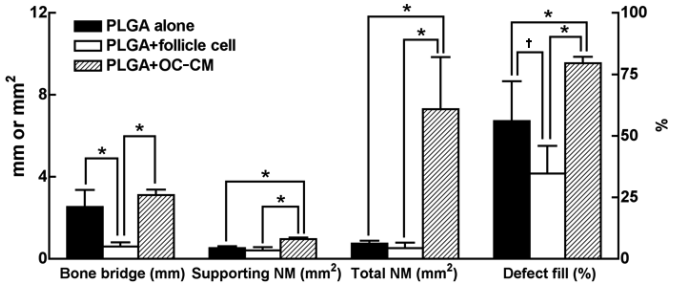

Figure 5.
*Histomorphometric analysis of periodontal regeneration: length of new bone bridge, area of supporting newly formed mineralized tissue (NM), area of total NM, and defect fill. Defects treated with carrier alone and carrier + cementoblasts show significantly greater bone defect bridging than those treated with carrier + follicle cells (*P <0.01). The carrier + cementoblasts group significantly promotes periodontal repair in comparison to the other two groups, in terms of area of total NM, area of supporting NM, and defect fill (*P <0.01). The carrier-alone group exhibits more new bone than the carrier + follicle cells group (†P <0.05).*

periodontal defects in rats, dogs, and non-human primates,[19,20,24,25] but in this study, such regeneration was achieved using cementoblasts alone, with no added factors. Most likely this is a result of cementoblast-mediated formation of a matrix conducive to cementogenesis. Ongoing research by our group and others is targeted at defining the specific genes/proteins of cementoblasts that regulate mineral formation.

In contrast to these results, the presence of follicle cells inhibited periodontal healing when compared to implants retrieved from mice receiving PLGA/cementoblast or PLGA control implants. This supports our studies in SCID mice where follicle cells were delivered ectopically via type I collagen/calcium phosphate sponges or PLGA carriers and no mineral formation was induced, while cementoblasts similarly implanted showed marked mineralization[11-13] (and unpublished data). These results are in conflict with results in vitro. Dental follicle cells differentiate toward a cementoblastic/osteoblastic phenotype in vitro as exhibited by induction of BSP/OCN mRNA and promotion of mineral formation when exposed to BMP-2 protein.[26] The difference in results between these in vivo and in vitro studies are significant and need to be considered when designing regenerative therapies.

This rat periodontal defect model, as used by King's group[19,20] and our group,[27] has proven to be a valuable model in studying periodontal healing. Although this model does not represent a critical-size defect for periodontal regeneration, it serves as a reasonable screening model to examine wound healing kinetics. The rate of defect healing appears slower in immunocompetent animals possessing intact T- and B-cell responses, such as Lewis rats.[27] T cell-mediated rejection has been suggested to be responsible for decreased vascularization and mineralization of allogeneic bone grafts,[28] but it is not clear whether it is associated with the fast self-healing of athymic rats. Another phenomenon noted in this study is the tumorogenesis related to immortalized cementoblasts. While it is not difficult to understand the cellular change, since these cells were immortalized with SV40 TAg, this phenomenon has not been observed when the same cells were implanted into SCID mice (up to 9 weeks), raising the speculation that it may be linked to rats lacking an immune response. It is also interesting to see that such neoplastic changes occurred only at the superficial portion of the implantation, and the deeper portion near the teeth had the same histological appearance to other cementoblast-treated, but tumor-free regions. Additional studies using larger animal model systems are needed to determine the feasibility of cell therapy.[23]

From the present study, we conclude that murine cementoblasts delivered via polymer sponges have a marked ability to repair periodontal defects by forming mineralized tissues in vivo, and that implanted primary follicle cells inhibit periodontal healing. Further studies examining the positive and negative factors secreted by cementoblasts and follicle cells can give clues to the balance of elements required for effective periodontal regeneration.

ACKNOWLEDGMENTS

The authors thank Dr. Daniel J. Chiego, University of Michigan School of Dentistry, for kindly providing the surgical microscope and Mr. Christopher Strayhorn, University of Michigan School of Dentistry, for his technical support in histology examination. This study was supported by USPHS Research Grants R01-DE13047 (MJS) and DE13397 (WVG and MJS) from the National Institute of Dental and Craniofacial Research, Bethesda, Maryland.

REFERENCES

1. Giannobile WV, Meraw SJ. Periodontal applications. In: Atala A, Lanza RP, eds. *Methods of Tissue Engineering*. San Diego: Academic Press; 2002:1205-1215.
2. Saygin NE, Giannobile WV, Somerman MJ. Molecular and cell biology of cementum. *Periodontol 2000* 2000;24: 73-98.
3. Bartold PM, McCulloch CA, Narayanan AS, Pitaru S. Tissue engineering: A new paradigm for periodontal regeneration based on molecular and cell biology. *Periodontol 2000* 2000;24:253-269.
4. Wikesjö UM, Selvig KA. Periodontal wound healing and regeneration. *Periodontol 2000* 1999;19:21-39.
5. Cochran DL, Wozney JM. Biological mediators for periodontal regeneration. *Periodontol 2000* 1999;19:40-58.
6. Becker W, Becker BE. Periodontal regeneration: A contemporary re-evaluation. *Periodontol 2000* 1999;19: 104-114.
7. Ripamonti U, Reddi AH. Tissue engineering, morphogenesis, and regeneration of the periodontal tissues by bone morphogenetic proteins. *Crit Rev Oral Biol Med* 1997;8:154-163.

8. Ouyang H, McCauley LK, Berry JE, D'Errico JA, Strayhorn CL, Somerman MJ. Response of immortalized murine cementoblasts/periodontal ligament cells to parathyroid hormone and parathyroid hormone-related protein in vitro. *Arch Oral Biol* 2000;45:293-303.
9. Tokiyasu Y, Takata T, Saygin E, Somerman M. Enamel factors regulate expression of genes associated with cementoblasts. *J Periodontol* 2000;71:1829-1839.
10. Hakki SS, Berry JE, Somerman MJ. The effect of enamel matrix protein derivative on follicle cells in vitro. *J Periodontol* 2001;72:679-687.
11. Somerman MJ, Ouyang HJ, Berry JE, et al. Evolution of periodontal regeneration: From the root's point of view. *J Periodont Res* 1999;34:420-424.
12. Jin QM, Zhao M, Webb SA, Berry JE, Somerman MJ, Giannobile WV. Cementum engineering with three-dimensional polymer scaffolds. *J Biomed Mater Res* 2003;67A:54-60.
13. Saygin NE, Tokiyasu Y, Giannobile WV, Somerman MJ. Growth factors regulate expression of mineral-associated genes in cementoblasts. *J Periodontol* 2000;71:1591-1600.
14. Krebsbach PH, Gu K, Franceschi RT, Rutherford RB. Gene therapy-directed osteogenesis: BMP-7-transduced human fibroblasts form bone in vivo. *Hum Gene Ther* 2000;11:1201-1210.
15. Wise GE, Lin F, Fan W. Culture and characterization of dental follicle cells from rat molars. *Cell Tissue Res* 1992; 267:483-492.
16. Chen D, Chen H, Feng JQ, et al. Osteoblastic cells lines derived from a transgenic mouse containing the osteocalcin promoter driving SV40 T-antigen. *Mol Cell Differentiation* 1995;3:193-212.
17. D'Errico JA, Berry JE, Ouyang H, Strayhorn CL, Windle JJ, Somerman MJ. Employing a transgenic animal model to obtain cementoblasts in vitro. *J Periodontol* 2000;71:63-72.
18. Mooney DJ, Sano K, Kaufmann PM, et al. Long-term engraftment of hepatocytes transplanted on biodegradable polymer sponges. *J Biomed Mater Res* 1997;37:413-420.
19. King GN, King N, Cruchley AT, Wozney JM, Hughes FJ. Recombinant human bone morphogenetic protein-2 promotes wound healing in rat periodontal fenestration defects. *J Dent Res* 1997;76:1460-1470.
20. King GN, Hughes FJ. Bone morphogenetic protein-2 stimulates cell recruitment and cementogenesis during early wound healing. *J Clin Periodontol* 2001;28:465-475.
21. D'Errico JA, MacNeil RL, Takata T, Berry JE, Strayhorn C, Somerman MJ. Expression of bone associated markers by tooth root lining cells, in situ and in vitro. *Bone* 1997; 20:117-126.
22. Young MF, Ibaraki K, Kerr JM, Lyu MS, Kozak CA. Murine bone sialoprotein (BSP): cDNA cloning, mRNA expression, and genetic mapping. *Mamm Genome* 1994; 5:108-111.
23. Celeste AJ, Rosen V, Buecker JL, Kriz R, Wang EA, Wozney JM. Isolation of the human gene for bone gla protein utilizing mouse and rat cDNA clones. *EMBO J* 1986;5:1885-1890.
24. Giannobile WV, Finkelman RD, Lynch SE. Comparison of canine and non-human primate animal models for periodontal regenerative therapy: Results following a single administration of PDGF/IGF-I. *J Periodontol* 1994;65: 1158-1168.
25. Giannobile WV, Ryan S, Shih MS, Su DL, Kaplan PL, Chan TC. Recombinant human osteogenic protein-1 (OP-1) stimulates periodontal wound healing in Class III furcation defects. *J Periodontol* 1998;69:129-137.
26. Zhao M, Berry JE, Xiao G, Franceschi RT, Reddi A, Somerman MJ. BMP-2 induces dental follicle cells to differentiate toward a cementoblast/osteoblast phenotype. *J Bone Miner Res* 2002;17:1441-1451.
27. Jin QM, Anusaksathien O, Webb SA, Rutherford RB, Giannobile WV. Bone morphogenetic protein gene therapy for periodontal tissue engineering. *J Periodontol* 2003;74:202-213.
28. Kirkeby OJ, Nordsletten L, Skjeldal S. Healing of cortical bone grafts in athymic rats. *Acta Orthop Scand* 1992;63: 318-322.

Correspondence: Dr. Martha J. Somerman, University of Washington, School of Dentistry, P.O. Box 356365, 1959 NE Pacific, HSC D-322, Seattle, WA 98195-6365. Fax: 206/616-2612; e-mail: somerman@u.washington.edu.

Accepted for publication June 11, 2003.